# ADCN: An Anisotropic Density-Based Clustering Algorithm for Discovering Spatial Point Patterns with Noise

**Abstract**

Density-based clustering algorithms such as DBSCAN have been widely used for spatial knowledge discovery as they offer several key advantages compared to other clustering algorithms. They can discover clusters with arbitrary shapes, are robust to noise and do not require prior knowledge (or estimation) of the number of clusters. The idea of using a scan circle centered at each point with a search radius *Eps* to find at least *MinPts* points as a criterion for deriving local density is easily understandable and sufficient for exploring isotropic spatial point patterns. However, there are many cases that cannot be adequately captured this way, particularly if they involve linear features or shapes with a continuously changing density such as a spiral. In such cases, DBSCAN tends to either create an increasing number of small clusters or add noise points into large clusters. Therefore, in this paper, we propose a novel anisotropic density-based clustering algorithm (ADCN). To motivate our work, we introduce synthetic and real-world cases that cannot be sufficiently handled by DBSCAN (and OPTICS). We then present our clustering algorithm and test it with a wide range of cases. We demonstrate that our algorithm can perform as equally well as DBSCAN in cases that do not explicitly benefit from an anisotropic perspective and that it outperforms

DBSCAN in cases that do. Finally, we show that our approach has the same time complexity as DBSCAN and OPTICS, namely O(n log n) when using a spatial index and O($n^2$) otherwise. We provide an implementation and test the runtime over multiple cases.

*Keywords:* Anisotropic, clustering, noise, spatial point patterns

---

## 1. Introduction and Motivation

Cluster analysis is a key component of modern knowledge discovery, be it as a technique for reducing dimensionality, identifying prototypes, cleansing noise, determining core regions, or segmentation. A wide range of clustering algorithms, such as DBSCAN (Ester et al., 1996), OPTICS (Ankerst et al., 1999), K-means (MacQueen et al., 1967), and Mean Shift (Comaniciu and Meer, 2002), have been proposed and implemented over the last decades. Many clustering algorithms depend on *distance* as their main criterion (Davies and Bouldin, 1979). They assume *isotropic* second-order effects (i.e., spatial dependence) among spatial objects thereby implying that the magnitude of similarity and interaction between two objects mostly depends on their distance. However, the genesis of many geographic phenomena demonstrates clear *anisotropic* spatial processes. As for ecological and geological features, such as the spatial distribution of rocks (Hoek, 1964), soil (Barden, 1963), and airborne pollution (Isaaks and Srivastava, 1989), their spatial patterns vary in direction (Fortin et al., 2002). Similarly, data about urban dynamics from social media, the census, transportation studies, and so forth, are highly restricted and defined by the layout of urban spaces, and thus show clear variance along directions. To give a concrete example, geotagged images be it in the city or the great outdoors, show clear directional patterns due to roads, hiking trails, or simply for the fact that they originate from human, goal-directed trajectories. Isotropic clustering algorithms such as DBSCAN have difficulties dealing with the resulting point patterns and either fail to eliminate noise or do so at the expense of introducing many small clusters. One such example is depicted in Figure 1. Due to the changing density, algorithms such as DBSCAN will classify some noise, i.e., points between the spiral arms, as being part of the cluster. To address this problem, we propose an anisotropic density-based clustering algorithm.

[Figure 1 about here.]

**More specifically, the research contributions of this paper are as follows:**

- We introduce an anisotropic density-based clustering algorithm (ADCN [1]). While the algorithm differs in the underlying assumptions, it uses the same two parameters as DBSCAN, namely *Eps* and *MinPts*, thereby providing an intuitive explanation and integration into existing workflows.

- We motivate the need for such algorithm by showing 12 synthetic and 8 real-world use cases and each with 3 different noise definitions modeled as buffers that generate a total of 60 test cases.

[1]This paper is a substantially extended version of the short paper Mai et al. (2016). It also adds an open source implementation of ADCN, a test environment, as well as new evaluation results on a larger sample.

- We demonstrate that ADCN performs as well as DBSCAN (and OPTICS) for isotropic cases but outperforms both algorithms in cases that benefit from an anisotropic perspective.

- We argue that ADCN has the same time complexity as DBSCAN and OPTICS, namely O(n log n) when using a spatial index and $O(n^2)$ otherwise.

- We provide an implementation for ADCN and apply it to the use cases to demonstrate the runtime behavior of our algorithm. As ADCN has to compute whether a point is within an ellipse instead of merely relying on the radius of the scan circle, its runtime is slower than DBSCAN while remaining comparable to OPTICS. We discuss how the runtime difference can be reduced by using a spatial index and by testing the radius case first.

The remainder of the paper is structured as follows. First, in Section 2, we discuss related work such as variants of DBSCAN. Next, we introduce ADCN and discuss two potential realizations of measuring anisotropicity in Section 3. Use cases, the development of a test environment, and a performance evaluation of ADCN are presented in Section 4. Finally, in Section 5, we conclude our work and point to directions for future work.

## 2. Related Work

Clustering algorithms can be classified into several categories, including but not limited to partitioning, hierarchical, density-based, graph-based, and grid-based approaches (Han et al., 2011; Deng et al., 2011). Each of these categories contains several well known clustering algorithms with their specific pros and cons. Here we focus on the density-based approaches.

Density-based clustering algorithms are widely used in big geo-data mining and analysis tasks, like generating polygons from a set of points (Moreira and Santos, 2007; Duckham et al., 2008; Zhong and Duckham, 2016), discovering urban areas of interest (Hu et al., 2015), revealing vague cognitive regions (Gao et al., 2017), detecting human mobility patterns (Huang and Wong, 2015; Huang, 2017; Huang and Wong, 2016; Jurdak et al., 2015), and identifying animal mobility patterns (Damiani et al., 2016).

Density-based clustering has many advantages over other approaches. These advantages include: 1) the ability to discover clusters with arbitrary shapes; 2) robustness to data noise; and 3) no requirement to pre-define the number of clusters. While DBSCAN remains the most popular density-based clustering method, many related algorithms have been proposed to compensate some of its limitations. Most of them, such as OPTICS (Ankerst et al., 1999) and VDBSCAN (Liu et al., 2007), address problems arising from density variations within clusters. Others, such as ST-DBSCAN (Birant and Kut, 2007), add a temporal dimension. GDBSCAN (Sander et al., 1998) extends DBSCAN to include non-spatial attributes into clustering and enables the clustering of high dimensional data. NET-DBSCAN (Stefanakis, 2007) revises DBSCAN for network data. To improve the computational efficiency, algorithms such as IDBSCAN (Borah and Bhattacharyya, 2004) and KIDBSCAN (Tsai and Liu, 2006) have been proposed.

All of these algorithms use distance as the major clustering criterion.

They assume that the observed spatial patterns are isotropic, i.e., that intensity dose not vary by direction. For example, DBSCAN uses a scan circle with an *Eps* radius centered at each point to evaluate the local density around the corresponding point. A cluster is created and expanded as long as the number of points inside this circle (*Eps*-neigborhood) is larger than *MinPts*. Consequently, DBSCAN does not consider the spatial distribution of the *Eps*-neigborhood which poses problems for linear patterns.

Some clustering algorithms do consider local directions. However, most of these so-call direction-based clustering techniques use spatial data which have a pre-defined local direction, e.g., trajectory data. The *local direction* of one point is pre-defined as the direction of the vector which is part of the trajectories with the corresponding point as its origination or destination. DEN (Zhou et al., 2010) is one direction-based clustering method which uses a grid data structure to group trajectories by moving directions. PDC+ (Wang and Wang, 2012) is another trajectory specific DBSCAN variant that includes the direction per point. DB-SMoT (Rocha et al., 2010) includes both the direction and temporal information of GPS trajectories from fishing vessel into the clustering process. Although all of these three direction-based clustering algorithms incorporate local direction as one of the clustering criteria, they can be applied to only trajectories data.

*Anisotropicity* (Fortin et al., 2002) describes the variation of directions in spatial point processes in contrast to *isotropicity*. It is another way to describe intensity variation in spatial point process other than first- and second-order effects. *Anisotropicity* has been studied in the context of interpolation where a spatially continuous phenomenon is measured, such as directional variogram (Isaaks and Srivastava, 1989) and different modifications of Kriging methods based on local anisotropicity (Stroet and Snepvangers, 2005; Machuca-Mory and Deutsch, 2013; Boisvert et al., 2009). In this paper we focus on *anisotropicity* of spatial point processes. Researchers studied *anisotropicity* of spatial point processes from a theoretical perspective by analyzing their realizations such as detecting anisotropy in spatial point patterns (DErcole and Mateu, 2013) and estimating geometric anisotropic spatial point patterns (Rajala et al., 2016; Møller and Toftaker, 2014). Here, we study *anisotropicity* in the context of density-based clustering algorithms.

A few clustering algorithms take anisotropic processes into account. For instance, in order to obtain good results for crack detection, an anisotropic clustering algorithm (Zhao et al., 2015) has been proposed to revise DBSCAN by changing the distance metric to geodesic distance. QUAC (Hanwell and Mirmehdi, 2014) demonstrates another anisotropic clustering algorithm which does not make an isotropic assumption. It takes the advantages of anisotropic Gaussian kernels to adapt to local data shapes and scales and prevents singularities from occurring by fitting the Gaussian mixture model (GMM). QUAC emphasizes the limitation of an isotropic assumption and highlights the power of anisotropic clustering. However, due to the use of anisotropic Gaussian kernels, QUAC can only detect clusters which have ellipsoid shapes. Each cluster derived from QUAC will have a major direction. In real-world cases, spatial pattern will show arbitrary shapes. Even more, the local direction is not necessary the same between and even within clusters. Instead, it is reasonable to assume that local direction can change continuously in different parts of the same cluster.

## 3. Introducing ADCN

In this section we introduce the proposed **A**nisotropic **D**ensity-based **C**lustering with **N**oise (ADCN).

### *3.1. Anisotropic Perspective on Local Density*

Without predefined direction information from spatial datasets, one has to compute the *local direction* for each point based on the spatial distribution of points around it. The standard deviation ellipse (SDE) (Yuill, 1971) is a suitable method to get the major direction of a point set. In addition to the major direction (long axis), the flattening of the SDE implies how much the points are strictly distributed along the long axis. The flattening of an ellipse is calculated from its long axis $a$ and short axis $b$ as given by Equation 1:

$$f = \frac{a-b}{a} \tag{1}$$

Given $n$ points, the standard deviation ellipse constructs an ellipse to represent the orientation and arrangement of these points. The center of this ellipse $O(\overline{X}, \overline{Y})$ is defined as the geometric center of these $n$ points and is calculated by Equation 2:

$$\overline{X} = \frac{\sum_{i=1}^{n} x_i}{n}, \overline{Y} = \frac{\sum_{i=1}^{n} y_i}{n} \tag{2}$$

The coordinates $(x_i, y_i)$ of each point are normalized to the deviation from the mean areal center point (Equation 3):

$$\widetilde{x_i} = x_i - \overline{X}, \widetilde{y_i} = y_i - \overline{Y}, \tag{3}$$

Equation 3 can be seen as a coordinates translation to the new origin ($\overline{X}$, $\overline{Y}$). If we rotate the new coordinate system counterclockwise about $O$ by angle $\theta$ ($0 < \theta \leqslant 2\pi$) and get the new coordinate system $X_o$-$Y_o$, the standard deviation along $X_o$ axis $\sigma_x$ and $Y_o$ axis $\sigma_y$ is calculated as given in Equation 4 and 5.

$$\sigma_x = \sqrt{\frac{\sum_{i=1}^{n}(\widetilde{y}_i \sin\theta + \widetilde{x}_i \cos\theta)^2}{n}} \tag{4}$$

$$\sigma_y = \sqrt{\frac{\sum_{i=1}^{n}(\widetilde{y}_i \cos\theta - \widetilde{x}_i \sin\theta)^2}{n}} \tag{5}$$

The long/short axis of SDE is along the direction who has the maximum/minimum standard deviation. Let $\sigma_{max}$ and $\sigma_{min}$ be the length the of semi-long axis and semi-short axis of SDE. The angle of rotation $\theta_m$ of the long/short axis is given by Equation 6 (Yuill, 1971).

$$\tan\theta_m = -\frac{A \pm B}{C} \tag{6}$$

$$A = \sum_{i=1}^{n} \widetilde{x}_i^{\,2} - \sum_{i=1}^{n} \widetilde{y}_i^{\,2} \tag{7}$$

$$C = 2\sum_{i=1}^{n} \widetilde{x}_i \widetilde{y}_i \tag{8}$$

$$B = \sqrt{A^2 + C^2} \tag{9}$$

The $\pm$ indicates two rotation angles $\theta_{max}$, $\theta_{min}$ corresponding to long and short axis.

### *3.2. Anisotropic Density-Based Clusters*

In order to introduce an anisotropic perspective to density-based clustering algorithms such as DBSCAN, we have to revise the definition of an

*Eps*-neighborhood of a point. First, the original *Eps*-neighborhood of a point in a dataset $D$ is defined by DBSCAN as given by Definition 1.

**Definition 1.** *(Eps-neighborhood of a point) The Eps-neighborhood $N_{Eps}(p_i)$ of Point $p_i$ is defined as all the points within the scan circle centered at $p_i$ with a radius Eps, which can be expressed as:*

$$N_{Eps}(p_i) = \{p_j(x_j, y_j) \in D | dist(p_i, p_j) \leqslant Eps\}$$

Such scan circle results in an isotropic perspective on clustering. However, as we discuss above, an anisotropic assumption will be more appropriate for some geographic phenomena. Intuitively, in order to introduce anisotropicity to DBSCAN, one can employ a scan ellipse instead of a circle to define the *Eps*-neighborhood of each point. Before we give a definition of the *Eps*-ellipse-neighborhood of a point, it is necessary to define a set of points around a point (Search-neighborhood of a point) which is used to derive the scan ellipse; See Definition 2.

**Definition 2.** *(Search-neighborhood of a point) A set of points $S(p_i)$ around Point $p_i$ is called search-neighborhood of Point $p_i$ and can be defined in two ways:*

1. *The Eps-neighborhood $N_{Eps}(p_i)$ of Point $p_i$.*
2. *The k-th nearest neighbor $KNN(p_i)$ of Point $p_i$. Here $k = MinPts$ and $KNN(p_i)$ does not include $p_i$ itself.*

After determining the search-neighborhood of a point, it is possible to define the *Eps*-ellipse-neighborhood region (See Definition 3) and *Eps*-ellipse-neighborhood (See Definition 4) of each point.

**Definition 3.** *(Eps-ellipse-neighborhood region of a point) An ellipse $ER_i$ is called Eps-ellipse-neighborhood region of a point $p_i$ iff:*

1. *Ellipse $ER_i$ is centered at Point $p_i$.*
2. *Ellipse $ER_i$ is scaled from the standard deviation ellipse $SDE_i$ computed from the Search-neighborhood $S(p_i)$ of Point $p_i$.*
3. $\frac{\sigma_{max}'}{\sigma_{min}'} = \frac{\sigma_{max}}{\sigma_{min}}$ *;*
   *where $\sigma_{max}'$,$\sigma_{min}'$ and $\sigma_{max}$,$\sigma_{min}$ are the length of semi-long and semi-short axis of Ellipse $ER_i$ and Ellipse $SDE_i$.*
4. $Area(ER_i) = \pi ab = \pi Eps^2$

According to Definition 3, the *Eps*-ellipse-neighborhood region of a point is computed based on the search-neighborhood of a point. Since there are two definitions of the search-neighborhood of a point (See Definition 2), each point should have a unique *Eps*-ellipse-neighborhood region given *Eps* (using the first definition in Definition 2) or $MinPts$ (using the second definition in Definition 2) as long as the search-neighborhood of the current point has at least two points for the computation of the standard deviation ellipse.

**Definition 4.** *(Eps-ellipse-neighborhood of a point) An Eps-ellipse-neighborhood $EN_{Eps}(p_i)$ of point $p_i$ is defined as all the point inside the eillpse $ER_i$, which can be expressed as* $EN_{Eps}(p_i) = \{p_j(x_j, y_j) \in D | \frac{((y_j - y_i)\sin\theta_{max} + (x_j - x_i)\cos\theta_{max})^2}{a^2} + \frac{((y_j - y_i)\cos\theta_{max} - (x_j - x_i)\sin\theta_{max})^2}{b^2} \leqslant 1\}$.

There are two kinds of points in a cluster obtained from DBSCAN: *core point* and *border point*. Core points have at least $MinPts$ points in their *Eps*-neighborhood, while border points have less than $MinPts$ points in their *Eps*-neighborhood but are *density reachable* from at least one core point. Our anisotropic clustering algorithm has a similar definition of core point and border point. The notions of directly anisotropic-density-reachable and core point are illustrated bellow; see Definition 5.

**Definition 5.** *(Directly anisotropic-density-reachable) A point $p_j$ is directly anisotropic density reachable from point $p_i$ wrt. Eps and $MinPts$ iff:*

1. $p_j \in EN_{Eps}(p_i)$.
2. $|EN_{Eps}(p_i)| \geqslant MinPts$. *(Core point condition)*

If point $p$ is directly anisotropic reachable from point $q$, then point $q$ must be a core point which has no less than $MinPts$ points in its *Eps*-ellipse-neighborhood. Similar to the notion of density-reachable in DBSCAN, the notion of anisotropic-density-reachable is given in Definition 6.

**Definition 6.** *(Anisotropic-density-reachable) A point $p$ is anisotropic density reachable from point $q$ wrt. Eps and $MinPts$ if there exists a chain of points $p_1$, $p_2$, ..., $p_n$, ($p_1 = q$, and $p_n = p$) such that point $p_{i+1}$ is directly anisotropic density reachable from $p_i$.*

Although anisotropic density reachability is not a symmetric relation, if such a directly anisotropic density reachable chain exits, then except for point $p_n$, the other $n-1$ points are all core points. If Point $p_n$ is also a core point, then symmetrically point $p_1$ is also density reachable from $p_n$. That means that if two points $p$, $q$ are anisotropic density reachable from each other, then both of them are core points and belong to the same cluster.

Equipped with the above definitions, we are able to define our anisotropic density-based notion of clustering. DBSCAN includes both core points and border points into its clusters. In our clustering algorithm, only core points will be treated as cluster points. Border points will be excluded from clusters and treated as noise points, because otherwise many noise points will be included into clusters according to experimental results. In short, a cluster (See definition 7) is defined as a subset of points from the whole points dataset in which each two points are anisotropic density reachable from another. Noise points (See Definition 8) are defined as the subset of points from the entire points dataset for which each point has less than $MinPts$ points in its $Eps$-ellipse-neighborhood.

**Definition 7.** *(Cluster) Let $D$ be a points dataset. A cluster $C$ is a no-empty subset of $D$ wrt. $Eps$ and $MinPts$, iff:*

1. $\forall p \in C$, $EN_{Eps}(p) \geqslant MinPts$.
2. $\forall p, q \in C$, *$p$, $q$ are anisotropic density reachable from each other wrt. $Eps$ and $MinPts$.*

A cluster $C$ has two attribute:

$\forall p \in C$ and $\forall q \in D$, if $p$ is anisotropic density reachable from $q$ wrt. $Eps$ and $MinPts$, then

1. $q \in C$.
2. There must be a directly anisotropic density reachable points chain $C(q, p)$: $p_1$, $p_2$, ..., $p_n$, ($p_1 = q$, and $p_n = p$), such that $p_{i+1}$ is directly anisotropic density reachable from $p_i$. Then $\forall p_i \in C(q, p)$, $p_i \in C$.

**Definition 8.** *(Noise) Let $D$ be a points dataset. A point $p$ is a noise point wrt. $Eps$ and $MinPts$, if $p \in D$ and $EN_{Eps}(p) < MinPts$.*

Let $C_1$, $C_2$, ..., $C_k$ be the clusters of the points dataset $D$ wrt. $Eps$ and $MinPts$. From Definition 8, if $p \in D$, and $EN_{Eps}(p) < MinPts$, then $\forall C_i \in \{C_1, C_2, ..., C_k\}$, $p \notin C_i$.

[Figure 2 about here.]

[Figure 3 about here.]

According to Definition 2, and in contrast to a simple scan circle, there are at least two ways to define a search neighborhood of the center point $p_i$. Thus, ADCN can be divided into a ADCN-Eps variant that uses $Eps$-neighborhood $N_{Eps}(p_i)$ as the search neighborhood and ADCN-KNN that uses k-th nearest neighbors $KNN(p_i)$ as the search neighborhood. Figures 2 and 3 illustrates the related definitions for ADCN-Eps and ADCN-KNN. The red points in both figures represent current center points. The blue points indicate the two different search neighborhoods of the corresponding center points according to Definition 2. Note that for ADCN-Eps, the center point is also part of its search neighborhood which is not true for ADCN-KNN. The green ellipses and green crosses stand for the standard deviation ellipses constructed from the corresponding search neighborhood and their center points. The red ellipses are $Eps$-ellipse-neighborhood regions while the dash line circles indicate a DBSCAN-like scan circle. As can be seen, ADCN-KNN will exclude the point to the left of the linear *bridge*-pattern while DBSCAN would include it.

### 3.3. ADCN Algorithms

From the definitions provided above it follows that our *anisotropic density-based clustering with noise* algorithm takes the same parameters ($MinPts$ and $Eps$) as DBSCAN and that they have to be decided before clustering. This is for good reasons, as the proper selection of DBSCAN parameters has been well studied and ADCN can easily replace DBSCAN without any changes to established workflows.

As shown in Algorithm 1, ADCN starts with an arbitrary point $p_i$ in a points dataset $D$ and discovers all the *core* points which are anisotropic density reachable from point $p_i$. According to Definition 2, there are two ways to get the search neighborhood of point $p_i$ which will result in different $Eps$-ellipse-neighborhood $EN_{Eps}(p_j)$ based on the derived $Eps$-ellipse-neighborhood-region in Algorithm 2. Hence, ADCN can be implemented by two algorithms (ADCN-Eps, ADCN-KNN). Algorithm 2 needs to take care of situations when all points of the Search-neighborhood $S(p_i)$ of Point $p_i$ are *strictly* on the same line. In this case, the short axis of $Eps$-ellipse-neighborhood region $ER_i$ becomes *zero* and its long axis become *Infinity*. This means $EN_{Eps}(p_i)$ is diminished to a straight line. The process of constructing $Eps$-ellipse-neighborhood $EN_{Eps}(p_i)$ of Point $p_i$ becomes a point-on-line query.

According to Algorithm 3, ADCN-Eps uses the $Eps$-neighborhood $N_{Eps}(p_i)$ of point $p_i$ as the search neighborhood which will be used later to construct the standard deviation ellipse. In contrast, ADCN-KNN (Algorithm 4) uses a k-th nearest neighborhood of point $p_i$ as the search neighborhood. Here point $p_i$ will not be included in its k-th nearest neighborhood. As can be seen, the run times of ADCN-Eps and ADCN-KNN are heavily dominated by the search-neighborhood query which is executed on each point. Hence, the time complexities of ADCN, DBSCAN, and OPTICS are O($n^2$) without a spatial index and O(n log n) otherwise.

## 4. Experiments and Performance Evaluation

In this section, we will evaluate the performance of ADCN from two perspectives: clustering quality and clustering efficiency. In contrast to the scan circle of DBSCAN, there are at least two ways to determine an anisotropic neighborhood. This leads to two realizations of ADCN, namely ADCN-KNN and ADCN-Eps. We will evaluate their performance using DBSCAN and OPTICS as baselines. We selected OPTICS as an additional baseline as it is commonly used to address some of DBSCAN's shortcomings with respect to varying densities.

According to the research contributions outlined in Section 1, we intend to establish **(1)** that at least one of the ADCN variants performs as good as DBSCAN (and OPTICS) for cases that do not explicitly benefit from an anisotropic perspective; **(2)** that the aforementioned variant performs better than the baselines for cases that *do* benefit from an anisotropic perspective; and finally **(3)** that the test cases include point patterns typically used to test density-based clustering algorithms as well as *real-world* cases that highlight the need for developing ADCN in the first place. In addition, we will show runtime results for all four algorithms.

### *4.1. Experiment Designs*

We have designed several spatial point patterns as test cases for our experiments. More specifically, we generated 20 test cases with 3 different noise settings for each of them. These consist of 12 synthetic and 8 real-world use cases which results in a total of **60** case studies. Note that our test cases do not only contain linear features such as road networks but also cases that are typically used to evaluate algorithms such as DBSCAN, e.g., clusters of ellipsoid and rectangular shapes.

In order to simulate a "ground truth" for the synthetic cases, we created polygons to indicate different clusters and randomly generated points within these polygons and outside of them. We took a similar approach for the eight real-world cases. The only difference is that the polygons for real world cases have been generated from buffer zones with a 3-meter radius of the real-world features, e.g., existing road networks. This allows us to simulate patterns that typically occur in geo-tagged social media data.

Although we use this approach to simulate the corresponding spatial point process, the distinction between clustered points and noise points in the resulting spatial point patterns may not be so obvious even from a human's perspective. To avoid cases in which it is unreasonable to expect algorithms and humans to differentiate between noise and pattern, we introduced a clipping buffer of 0m, 5m, and 10m. For comparison, the typical position accuracy of GPS sensors on smartphones and GPS collars for wildlife tracking is about 3-15 meters (Wing et al., 2005)(and can decline rapidly in urban canyons).

The generated spatial point patterns of 12 synthetic and 8 real-world use cases with 0m buffer distance are shown in the first column of Figure 5 and Figure 6. Note that in all test cases, points generated from different polygons are pre-labeled with different cluster IDs which are indicated by different colors in the first column of Figure 5 and Figure 6. Points generated outside polygons are pre-labeled as *noise* which are shown in *black*. These generated spatial point patterns serve as *ground truth* which are used in our clustering quality evaluation experiments.

In order to demonstrate the strengthen of ADCN, we need to compare the performance of ADCN with that of DBSCAN and OPTICS from two perspectives: clustering quality and clustering efficiency. The experiment designs are as follow:

- As for clustering quality evaluation, we use several clustering quality indices to quantify how good the clustering results are. In this work, we use Normalized Mutual Information (NMI) and the Rand Index. We will explain these two indices in detail in Section 4.3. We stepwise tested every possible parameter combinations of $Eps$, $MinPts$ computationally on each test case. For each clustering algorithm, we select the parameter combination which has the highest NMI or Rand index. By comparing the maximum of NMI and Rand index across different clustering algorithms in each test case, we can find out the best clustering technique.

- As for clustering efficiency evaluation, we generate spatial point patterns with different numbers of points by using the polygons of each test case mentioned earlier. For each clustering algorithm and each number of points setting, we computed the average runtime. By constructing a runtime curve of each clustering algorithm, we are able to compare their runtime efficiency.

### 4.2. Test Environment

In order to compare the performance of ADCN with that of DBSCAN and OPTICS, we developed a JavaScript test environment to generate patterns and compare the results. It allows us to generate use cases in a Web browser, such as Firefox or Chrome, or load them from a GIS, change noise settings, determine DBSCAN's Eps via a KNN distance plot, perform different evaluations, compute runtimes, index the data via an R-tree, and save and load the data. Consequently, what matters is the *runtime behavior*, not the exact performance (for which JavaScript would not be a suitable choice). All cases have been performed on a *cold* setting, i.e., without any caching using an Intel i5-5300U CPU with 8 GB RAM on an Ubuntu 16.04 system. This Javascript test environment as well as all the test cases can be downloaded from here[2].

Figure 4 shows a snapshot of this test environment. The system has two main panels. The map panel on the left side is an interactive canvas in which the user can click and create data points. The tool bar on the right side is composed of input boxes, selection boxes, and buttons which are divided into different groups. Each group is used for a specific purpose, which will be discussed as below.

[Figure 4 about here.]

[2] `http://stko.geog.ucsb.edu/adcn/`

The "File Operation" tool group is used for point dataset manipulation. For simplicity, our environment defines a simple format for point datasets. Conceptually, a point dataset is a table containing the coordinates of points, their ground truth memberships, and the memberships produced during the experiments. The ground truth and experimental memberships are then compared to evaluate the cluster algorithms. The "Open Pts File" box is used for loading point datasets produced by other GIS. The data points can also be abstract points which represent objects, such as documents (Fabrikant and Montello, 2008), in a feature space. The prototype takes the coordinates of points and maps out these points after rescaling their coordinates based on the size of the map panel. During the clustering process it uses Euclidean distance as the distance measure.

The "Clustering Operation" tool group is used to operate clustering tasks. The "Eps" and "MinPts" input boxes let users enter the clustering parameters for all clustering algorithms. The "DBSCAN", "OPTICS", "ADCN-Eps", "ADCN-KNN" buttons are for running the algorithms. As for the implementation of DBSCAN and OPTICS, we used a JavaScript clustering library from GitHub [3]. This library has basic implementations of DBSCAN, OPTICS, K-MEANS, and some other clustering algorithms without any spatial indexes. Our ADCN-KNN and ADCN-Eps algorithms were implemented using the same data structures as used in the library. Such an implementation ensures that the evaluation result will reflect the differences of the algorithms rather than be affected by the specific data structures used in the

[3] `https://github.com/uhho/density-clustering`

implementations. Finally, we implemented an R-tree spatial index to accelerate the neighborhood search. We have used the R-tree JavaScript library from GitHub [4].

The "Clustering Evaluation" tool group is composed of "Quality Evaluation" and "Efficiency Evaluation" subgroups. As for the clustering quality evaluation, we implemented two metrics, Normalized mutual Information (NMI) and Rand Index, to quantify the goodness of the clustering results. The first four buttons in this subgroup will run the corresponding clustering algorithm on the current dataset based on all possible parameter combinations. They will compute two clustering evaluation indexes for each clustering result. The "SAVE Index As..." button will save these results to a text file.

Efficiency evaluation is another important part for comparing clustering algorithms. The "Efficiency Evaluation" button will run these four clustering algorithms on datasets with different sizes. The "SAVE Efficiency Test As..." button can be further used to save the result into a text file.

Finally, the "KNN" tool group is used to draw the $k_{th}$ *nearest neighbor plot* (KNN plot) of the current dataset based on the *MinPts* parameter specified by the user. For each point, the KNN plot obtains the distance between the current point and its $k_{th}$ nearest point (here $K$ is *MinPts*). Then it ranks these $k_{th}$ nearest distance of each point in an ascending order. The KNN plot can be used for estimating the appropriate *Eps* for the current point dataset given *MinPts*. More details this estimation can be found in the original DBSCAN paper (Ester et al., 1996).

[4] `https://github.com/imbcmdth/RTree`

Note that we provide the test environment to make our results reproducible and to offer a reusable implementation of ADCN, without implying that JavaScript would be the language of choice for future, large-scale applications of ADCN.

### *4.3. Evaluation of Clustering Quality*

We use two clustering quality indices - the normalized mutual information (NMI) and the Rand Index - to measure the quality of clustering results of all algorithms. NMI originates from information theory and has been revised as an objective function for clustering ensembles (Strehl and Ghosh, 2002). NMI evaluates the accumulated mutual information shared by the clusters from different clustering algorithms. Let $n$ be the number of points in a point datasets $D$. $X = (X_1, X_2, ..., X_r)$ and $Y = (Y_1, Y_2, ..., Y_s)$ are two clustering results from the same or different clustering algorithms. Note that noise points will be treated as their own cluster. Let $n_h^{(x)}$ be the number of points in cluster $X_h$ and $n_l^{(y)}$ the number of points in cluster $Y_l$. Let $n_{h,l}^{(x,y)}$ be the number of points in the intersect of cluster $X_h$ and $Y_l$. Then the normalized mutual information $\Phi^{(NMI)}(X,Y)$ is defined in Equation 10 as the similarity between two clustering results $X$ and $Y$:

$$\Phi^{(NMI)}(X,Y) = \frac{\sum_{h=1}^{r}\sum_{l=1}^{s} n_{h,l}^{(x,y)} \log \frac{n \cdot n_{h,l}^{(x,y)}}{n_h^{(x)} \cdot n_l^{(y)}}}{\sqrt{(\sum_{h=1}^{r} n_h^{(x)} \log \frac{n_h^{(x)}}{n})(\sum_{l=1}^{s} n_l^{(y)} \log \frac{n_l^{(y)}}{n})}} \tag{10}$$

Rand Index (Rand, 1971) is another objective function for clustering ensembles from a different perspective. It evaluates to which degree two clustering algorithms share the same relationships between points. Let $a$ be the number of pairs of points in $D$ that are in the same clusters in $X$ and in the same cluster in $Y$. $b$ is the number of pairs of points in $D$ that are in different clusters in $X$ and $Y$. $c$ is the number of pairs of points in $D$ that are in the same clusters in $X$ and in different cluster in $Y$. Finally, $d$ is the number of pairs of points in $D$ that are in different clusters in $X$ and in the same cluster in $Y$. The Rand Index $\Phi^{(Rand)}(X, Y)$ is then defined as given by Equation 11:

$$\Phi^{(Rand)}(X, Y) = \frac{a + b}{a + b + c + d} \tag{11}$$

For both NMI and Rand index, larger values indicate higher similarity between two clustering results. If a ground truth is available, both NMI and Rand can be used to compute the similarity between the result of an algorithms and the corresponding ground truth. This is called the *extrinsic method* (Han et al., 2011).

We use the aforementioned 20 test cases to evaluate the clustering quality of DBSCAN, ADCN-Eps, ADCN-KNN, and OPTICS. All of these four algorithms take the same parameters ($Eps$, $MinPts$). As there are no established methods to determine the best overall parameter combination (we use KNN distance plots to estimate Eps) with respect to NMI and Rand Index, we stepwise tested every possible parameter combinations of $Eps$, $MinPts$ computationally. An interactive 3D visualization of the NMI and Rand index results with changing $Eps$ and $MinPts$ for the *spiral* case with 0m buffer distance can be accessed online [5]. Table 1 shows the maximum NMI and

[5] http://stko.geog.ucsb.edu/adcn/

Rand Index results for the four algorithms over all test cases. Note that for each case, the best parameter combination with the maximum NMI does not necessarily yields the maximum Rand Index. However, among all of these 60 cases, there are 39, 35, 27, 39 cases for DBSCAN, ADCN-Eps, ADCN-KNN, OPTICS in which the best parameter combination for the maximum NMI is also the maximum Rand Index. For those cases where parameter combinations of maximum NMI and maximum Rand do not match, their parameters tend to be close to each other because NMI and Rand values are changing continuously while $Eps$ and $MinPts$ increase. This indicates that NMI and Rand Index have a medium to high similarity in terms of measuring the clustering quality.

As for the 60 test cases, ADCN-KNN has a higher maximum NMI/Rand Index than DBSCAN in **55** cases and has a higher maximum NMI/Rand Index than OPTICS in **55** cases; see also Figures 7 and 8. Even more, ADCN-KNN has a higher maximum NMI/Rand Index than ADCN-Eps in **31** cases; see Table 2. This indicates that ADCN-KNN gives the best clustering results among the tested algorithms. Our test cases do not only contain linear features but also cases that are typically used to evaluate algorithms such as DBSCAN, e.g., clusters of ellipsoid and rectangular shapes. In fact, these are the only cases were DBSCAN slightly out-competes ADCN-KNN, i.e., the maximum NMI/Rand Index of ADCN-KNN and DBSCAN are comparable. Summing up, ADCN-KNN performs better than all other algorithms when dealing with anisotropic cases and equally well as DBSCAN for isotropic cases. In the following paragraphs, we will use ADCN-KNN and ADCN interchangeably.

Figure 5 and 6 show the point patterns as well as the best clustering results of all algorithms for the twelve synthesis cases and eight real-world cases without buffering, i.e., with the 0m buffer distance. By comparing best clustering results of these four algorithms, we can find some interesting patterns: 1) *Connecting clusters along local directions*: ADCN has a better ability to detect the local direction of spatial point patterns and connect the clusters along this direction; 2) *Noise filtering*: ADCN does better in filtering out noise points. A good example of *connecting clusters along local directions* is the *ellipseWidth* case in Figure 5. As for the thinnest cluster in the bottom, the other 3 algorithms except ADCN-KNN extract multiple clusters from these points while ADCN-KNN is able to "connect" these clusters to a single one. Many cases show the *noise filtering* advantage of ADCN. For example, the*bridge* case, the *multiBridge* case in Figure 5, and the*Brooklyn Bridge* case in Figure 6, reveal that ADCN is better at detecting and filtering out noise points along bridge-like features.

[Figure 5 about here.]

[Figure 6 about here.]

[Figure 7 about here.]

[Figure 8 about here.]

### *4.4. Evaluation of Clustering Efficiency*

Finally, this subsection discusses runtime differences of the four tested algorithms. Without a spatial index, the time complexity of all algorithms is O($n^2$). *Eps*-neighborhood queries consume the major part of the run time of density-based clustering algorithms (Ankerst et al., 1999), and, therefore, also of ADCN-KNN and ADCN-Eps in terms of *Eps*-ellipse-neighborhood queries. Hence, we implemented an R-tree to accelerate the neighborhood queries for all algorithms. This changes their time complexity to O(n log n).

[Figure 9 about here.]

In order to enable a comprehensible comparison of the run times of all algorithms on different sizes of point datasets, we performed a batch of performance tests. The polygons from the 20 cases shown above have been used to generated point datasets of different sizes ranging from 500 to 10000 in 500 step intervals. The ratio of noise points to cluster points is set to 0.25. $Eps$, $MinPts$ are set to 15, 5 for all of these experiments. The average run times for the same size of point datasets is depicted in Figure 9.

Unsurprisingly, the runtime of all algorithms increases as the number of points increases. The runtime of ADCN-KNN is larger than that of DBSCAN and similar that of OPTICS. As the size of the point dataset increases, the ratio of the runtimes of ADCN-KNN to DBSCAN decrease from 2.80 to 1.29. The original OPTICS paper states a 1.6 runtime factor compared to DBSCAN. The used OPTICS library failed on datasets exceeding 5500 points. We also fit the runtime data to the $xlog(x)$ function. Figure 9 shows the fitted curves and functions of each clustering algorithm. We can see that all $R^2$ of these functions are larger than 0.95 which means that the $xlog(x)$ function well captures the trends of the real runtime data of these clustering algorithms. For ADCN, our implementation tests for point-in-circle for the radius of the major axis before computing point-in-ellipse to significantly reduce the runtime. Further implementation optimizations are possible but out of scope of this paper.

## 5. Summary and Outlook

In this work, we proposed an anisotropic density-based clustering algorithm (ADCN). Both synthetic and real-world cases have been used to verify the clustering quality and efficiency of our algorithm compared to DBSCAN and OPTICS. We demonstrate that ADCN-KNN outperforms DBSCAN and OPTICS for the detection of anisotropic spatial point patterns and performs equally well in cases that do not explicitly benefit from an anisotropic perspective. ADCN has the same time complexity as DBSCAN and OPTICS, namely O(n log n) when using a spatial index and O($n^2$) otherwise. With respect to the average runtime, the performance of ADCN is comparable to OPTICS. Our algorithm is particularly suited for linear features such as typically encountered in urban structures. Application areas include but are not limited to cleaning and clustering geotagged social media data, e.g., from Twitter, Flickr or Strava, analyzing trajectories collected from car sensors, wildlife tracking, and so forth. Future work will focus on improving the implementation of ADCN as well as on studying cognitive aspects of clustering and noise detection of linear features.

## References

Ankerst, M., Breunig, M. M., Kriegel, H.-P., Sander, J., 1999. OPTICS: ordering points to identify the clustering structure. In: Proceedings of

ACM SIGMOD Conference. Vol. 28. ACM, pp. 49–60.

Barden, L., 1963. Stresses and displacements in a cross-anisotropic soil. Geotechnique 13 (3), 198–210.

Birant, D., Kut, A., 2007. ST-DBSCAN: An algorithm for clustering spatial–temporal data. Data & Knowledge Engineering 60 (1), 208–221.

Boisvert, J., Manchuk, J., Deutsch, C., 2009. Kriging in the presence of locally varying anisotropy using non-euclidean distances. Mathematical Geosciences 41 (5), 585–601.

Borah, B., Bhattacharyya, D., 2004. An improved sampling-based DBSCAN for large spatial databases. In: Proceedings of International Conference on Intelligent Sensing and Information. IEEE, pp. 92–96.

Comaniciu, D., Meer, P., 2002. Mean shift: A robust approach toward feature space analysis. IEEE Transactions on Pattern Analysis and Machine Intelligence 24 (5), 603–619.

Damiani, M. L., Issa, H., Fotino, G., Heurich, M., Cagnacci, F., 2016. Introducing presenceand stationarity indexto study partial migration patterns: an application of a spatio-temporal clustering technique. International Journal of Geographical Information Science 30 (5), 907–928.

Davies, D. L., Bouldin, D. W., 1979. A cluster separation measure. IEEE Transactions on Pattern Analysis and Machine Intelligence (2), 224–227.

Deng, M., Liu, Q., Cheng, T., Shi, Y., 2011. An adaptive spatial clustering algorithm based on delaunay triangulation. Computers, Environment and Urban Systems 35 (4), 320–332.

Duckham, M., Kulik, L., Worboys, M., Galton, A., 2008. Efficient generation of simple polygons for characterizing the shape of a set of points in the plane. Pattern Recognition 41 (10), 3224–3236.

DErcole, R., Mateu, J., 2013. On wavelet-based energy densities for spatial point processes. Stochastic environmental research and risk assessment 27 (6), 1507–1523.

Ester, M., Kriegel, H.-P., Sander, J., Xu, X., 1996. A density-based algorithm for discovering clusters in large spatial databases with noise. In: Proceedings of 2nd International Conference on KDD. Vol. 96. pp. 226–231.

Fabrikant, S. I., Montello, D. R., 2008. The effect of instructions on distance and similarity judgements in information spatializations. International Journal of Geographical Information Science 22 (4), 463–478.

Fortin, M.-j., Dale, M. R., Ver Hoef, J. M., 2002. Spatial analysis in ecology. Encyclopedia of environmetrics.

Gao, S., Janowicz, K., Montello, D. R., Hu, Y., Yang, J.-A., McKenzie, G., Ju, Y., Gong, L., Adams, B., Yan, B., 2017. A data-synthesis-driven method for detecting and extracting vague cognitive regions. International Journal of Geographical Information Science 31 (6), 1245–1271.

Han, J., Kamber, M., Pei, J., 2011. Data mining: concepts and techniques. Elsevier.

Hanwell, D., Mirmehdi, M., 2014. QUAC: Quick unsupervised anisotropic clustering. Pattern Recognition 47 (1), 427–440.

Hoek, E., 1964. Fracture of anisotropic rock. Journal of the South African Institute of Mining and Metallurgy 64 (10), 501–523.

Hu, Y., Gao, S., Janowicz, K., Yu, B., Li, W., Prasad, S., 2015. Extracting and understanding urban areas of interest using geotagged photos. Computers, Environment and Urban Systems 54, 240–254.

Huang, Q., 2017. Mining online footprints to predict users next location. International Journal of Geographical Information Science 31 (3), 523–541.

Huang, Q., Wong, D. W., 2015. Modeling and visualizing regular human mobility patterns with uncertainty: an example using twitter data. Annals of the Association of American Geographers 105 (6), 1179–1197.

Huang, Q., Wong, D. W., 2016. Activity patterns, socioeconomic status and urban spatial structure: what can social media data tell us? International Journal of Geographical Information Science 30 (9), 1873–1898.

Isaaks, E. H., Srivastava, R. M., 1989. Applied geostatistics. No. 551.72 I86. Oxford University Press.

Jurdak, R., Zhao, K., Liu, J., AbouJaoude, M., Cameron, M., Newth, D., 2015. Understanding human mobility from twitter. PloS one 10 (7), e0131469.

Liu, P., Zhou, D., Wu, N., 2007. VDBSCAN: varied density based spatial clustering of applications with noise. In: 2007 International conference on service systems and service management. IEEE, pp. 1–4.

Machuca-Mory, D. F., Deutsch, C. V., 2013. Non-stationary geostatistical modeling based on distance weighted statistics and distributions. Mathematical Geosciences 45 (1), 31–48.

MacQueen, J., et al., 1967. Some methods for classification and analysis of multivariate observations. In: Proceedings of the fifth Berkeley symposium on mathematical statistics and probability. Vol. 1. Oakland, CA, USA., pp. 281–297.

Mai, G., Janowicz, K., Hu, Y., Gao, S., 2016. Adcn: an anisotropic density-based clustering algorithm. In: Proceedings of the 24th ACM SIGSPATIAL International Conference on Advances in Geographic Information Systems. ACM, p. 58.

Møller, J., Toftaker, H., 2014. Geometric anisotropic spatial point pattern analysis and cox processes. Scandinavian Journal of Statistics 41 (2), 414–435.

Moreira, A., Santos, M. Y., 2007. Concave hull: A k-nearest neighbours approach for the computation of the region occupied by a set of points. In: Proceedings of the International Conference on Computer Graphics Theory and Applications. pp. 61–68.

Rajala, T. A., Särkkä, A., Redenbach, C., Sormani, M., 2016. Estimating geometric anisotropy in spatial point patterns. Spatial Statistics 15, 100–114.

Rand, W. M., 1971. Objective criteria for the evaluation of clustering methods. Journal of the American Statistical association 66 (336), 846–850.

Rocha, J. A. M., Times, V. C., Oliveira, G., Alvares, L. O., Bogorny, V., 2010. DB-SMoT: A direction-based spatio-temporal clustering method. In: 2010 5th IEEE International Conference Intelligent Systems. IEEE, pp. 114–119.

Sander, J., Ester, M., Kriegel, H.-P., Xu, X., 1998. Density-based clustering in spatial databases: The algorithm GDBSCAN and its applications. Data mining and knowledge discovery 2 (2), 169–194.

Stefanakis, E., 2007. NET-DBSCAN: clustering the nodes of a dynamic linear network. International Journal of Geographical Information Science 21 (4), 427–442.

Strehl, A., Ghosh, J., 2002. Cluster ensembles—a knowledge reuse framework for combining multiple partitions. Journal of machine learning research 3 (Dec), 583–617.

Stroet, C. B. t., Snepvangers, J. J., 2005. Mapping curvilinear structures with local anisotropy kriging. Mathematical geology 37 (6), 635–649.

Tsai, C.-F., Liu, C.-W., 2006. KIDBSCAN: a new efficient data clustering algorithm. In: International Conference on Artificial Intelligence and Soft Computing. Springer, pp. 702–711.

Wang, J., Wang, X., 2012. A spatial clustering method for points-with-directions. In: Rough Sets and Knowledge Technology. Springer, pp. 194–199.

Wing, M. G., Eklund, A., Kellogg, L. D., 2005. Consumer-grade global positioning system (gps) accuracy and reliability. Journal of forestry 103 (4), 169–173.

Yuill, R. S., 1971. The standard deviational ellipse; an updated tool for spatial description. Geografiska Annaler. Series B, Human Geography 53 (1), 28–39.

Zhao, G., Wang, T., Ye, J., 2015. Anisotropic clustering on surfaces for crack extraction. Machine Vision and Applications 26 (5), 675–688.

Zhong, X., Duckham, M., 2016. Characterizing the shapes of noisy, non-uniform, and disconnected point clusters in the plane. Computers, Environment and Urban Systems 57, 48–58.

Zhou, W., Xiong, H., Ge, Y., Yu, J., Ozdemir, H. T., Lee, K. C., 2010. Direction clustering for characterizing movement patterns. In: IRI. pp. 165–170.

**Algorithm 1:** ADCN($D$, $MinPts$, $Eps$)

**Input :** A set of n points $D(X, Y)$ ; $MinPts$; $Eps$;

**Output:** Clusters with different labels $C_i[]$; A set of noise points $Noi[]$

**foreach** *point* $p_i(x_i, y_i)$ *in the set of points* $D(X, Y)$ **do**
    Mark $p_i$ as *Visited*;
    //Get $Eps$-ellipse-neighborhood $EN_{Eps}(p_i)$ of $p_i$
    ellipseRegionQuery($p_i$, $D$, $MinPts$, $Eps$);
    **if** $|EN_{Eps}(p_i)| < MinPts$ **then**
        Add $p_i$ to the noise set $Noi[]$;
    **else**
        Create a new Cluster $C_i[]$;
        Add $p_i$ to $C_i[]$;
        **foreach** *point* $p_j(x_j, y_j)$ *in* $EN_{Eps}(p_i)$ **do**
            **if** $p_j$ *is not visited* **then**
                Mark $p_j$ as visited;
                //Get $Eps$-ellipse-neighborhood $EN_{Eps}(p_j)$ of Point $p_j$
                ellipseRegionQuery($p_j$, $D$, $MinPts$, $Eps$);
                **if** $|EN_{Eps}(p_j)| \geqslant MinPts$ **then**
                    Let $EN_{Eps}(p_i)$ as the merged set of $EN_{Eps}(p_i)$ and $EN_{Eps}(p_j)$;
                    Add $p_j$ to current cluster $C_i[]$;
                **else**
                    Add $p_j$ to the noise set $Noi[]$;
                **end**
            **end**
        **end**
    **end**
**end**

**Algorithm 2:** ellipseRegionQuery($p_i$, $D$, $MinPts$, $Eps$)

**Input :** $p_i$, $D$, $MinPts$, $Eps$

**Output:** $Eps$-ellipse-neighborhood $EN_{Eps}(p_i)$ of Point $p_i$

//Get the Search-neighborhood $S(p_i)$ of Point $p_i$. ADCN-Eps and ADCN-KNN use different functions.

ADCN-Eps: searchNeighborhoodEps($p_i$, $D$, $Eps$); ADCN-KNN: searchNeighborhoodKNN($p_i$, $D$, $MinPts$);

Compute the standard deviation ellipse $SDE_i$ base on the Search-neighborhood $S(p_i)$ of Point $p_i$;

Scale Ellipse $SDE_i$ to get the $Eps$-ellipse-neighborhood region $ER_i$ of Point $p_i$ to make sure $Area(ER_i) = \pi \times Eps^2$;

**if** *The length of short axis of* $ER_i == 0$ **then**

  // the $Eps$-ellipse-neighborhood region $ER_i$ of Point $p_i$ is diminished to a straight line. Get $Eps$-ellipse-neighborhood $EN_{Eps}(p_i)$ of Point $p_i$ by finding all points on this straight line $ER_i$;

**else**

  // the $Eps$-ellipse-neighborhood region $ER_i$ of Point $p_i$ is an ellipse. Get $Eps$-ellipse-neighborhood $EN_{Eps}(p_i)$ of Point $p_i$ by finding all the points inside Ellipse $ER_i$;

**end**

return $EN_{Eps}(p_i)$;

**Algorithm 3:** searchNeighborhoodEps($p_i$, $D$, $Eps$)

**Input** : $p_i$, $D$, $Eps$

**Output:** the Search-neighborhood $S(p_i)$ of Point $p_i$

// This function is used in ADCN-Eps // Get all the points whose distance from Point $p_i$ is less than $Eps$

**foreach** *point* $p_j(x_j, x_j)$ *in the set of points* $D(X, Y)$ **do**

  **if** $\sqrt{(x_i - x_j)^2 + (y_i - y_j)^2} \leqslant Eps$ **then**

    Add Point $p_j$ to $S(p_i)$;

**end**

return $S(p_i)$;

**Algorithm 4:** searchNeighborhoodKNN($p_i$,$D$,$MinPts$)

**Input :** $p_i$; $D$; $MinPts$

**Output:** the Search-neighborhood $S(p_i)$ of Point $p_i$

// This function is used in ADCN-KNN // Get the Kth nearest neighbor of Point $p_i$ excluding $p_i$ itself

KNNArray = new Array($MinPts$);

distanceArray = new Array($|D|$);

KNNLabelArray = new Array($|D|$);

**foreach** *point* $p_j(x_j, y_j)$ *in the set of points* $D(X, Y)$ **do**

  KNNLabelArray[j] = 0;

  distanceArray[j] = $\sqrt{(x_i - x_j)^2 + (y_i - y_j)^2}$;

  **if** $j == i$ **then**

    KNNLabelArray[j] = 1;

**end**

**foreach** *k in 0:*$(MinPts - 1)$ **do**

  minDist = Infinity;

  minDistID = 0;

  **foreach** *j in 0:*$|D|$ **do**

    **if** *KNNLabelArray[j] != 1* **then**

      **if** *minDist* $>$ *distanceArray[j]* **then**

        minDist = distanceArray[j];

        minDistID = j;

  **end**

  KNNLabelArray[minDistID] = 1;

  KNNArray[k] = minDistID;

  Add the point with minDistID as ID to $S(p_i)$;

**end**

return $S(p_i)$;

Table 1: Clustering quality comparisons

| | | NMI | | | | Rand | | | |
|---|---|---|---|---|---|---|---|---|---|
| Case | Buffer | DBSCAN | ADCN-Eps | ADCN-KNN | OPTICS | DBSCAN | ADCN-Eps | ADCN-KNN | OPTICS |
| bridge | 0m | 0.937 | 0.957 | 0.957 | 0.937 | 0.985 | 0.991 | 0.992 | 0.985 |
| | 5m | 0.948 | 0.966 | 0.967 | 0.949 | 0.989 | 0.993 | 0.994 | 0.989 |
| | 10m | 0.938 | 0.973 | 0.968 | 0.944 | 0.988 | 0.995 | 0.995 | 0.989 |
| circle | 0m | 0.864 | 0.865 | 0.912 | 0.864 | 0.955 | 0.964 | 0.978 | 0.955 |
| | 5m | 0.859 | 0.897 | 0.916 | 0.859 | 0.955 | 0.974 | 0.978 | 0.955 |
| | 10m | 0.864 | 0.911 | 0.923 | 0.864 | 0.960 | 0.979 | 0.982 | 0.960 |
| circleNarrow | 0m | 0.914 | 0.951 | 0.958 | 0.914 | 0.974 | 0.988 | 0.991 | 0.974 |
| | 5m | 0.939 | 0.946 | 0.965 | 0.939 | 0.983 | 0.987 | 0.993 | 0.983 |
| | 10m | 0.923 | 0.962 | 0.962 | 0.923 | 0.976 | 0.991 | 0.992 | 0.976 |
| circleRoad | 0m | 0.689 | 0.704 | 0.725 | 0.689 | 0.934 | 0.945 | 0.952 | 0.934 |
| | 5m | 0.737 | 0.758 | 0.779 | 0.737 | 0.950 | 0.963 | 0.962 | 0.951 |
| | 10m | 0.730 | 0.778 | 0.821 | 0.730 | 0.946 | 0.963 | 0.971 | 0.946 |
| curve | 0m | 0.918 | 0.946 | 0.955 | 0.918 | 0.978 | 0.989 | 0.991 | 0.978 |
| | 5m | 0.924 | 0.947 | 0.956 | 0.924 | 0.980 | 0.990 | 0.992 | 0.980 |
| | 10m | 0.916 | 0.943 | 0.947 | 0.916 | 0.978 | 0.988 | 0.989 | 0.978 |
| ellipse | 0m | 0.978 | 0.982 | 0.976 | 0.978 | 0.996 | 0.997 | 0.995 | 0.996 |
| | 5m | 0.979 | 0.982 | 0.980 | 0.979 | 0.996 | 0.997 | 0.996 | 0.996 |
| | 10m | 0.975 | 0.980 | 0.978 | 0.974 | 0.996 | 0.997 | 0.996 | 0.996 |
| ellipseWidth | 0m | 0.917 | 0.935 | 0.935 | 0.917 | 0.985 | 0.989 | 0.988 | 0.985 |
| | 5m | 0.919 | 0.933 | 0.939 | 0.919 | 0.988 | 0.989 | 0.989 | 0.988 |
| | 10m | 0.931 | 0.938 | 0.941 | 0.931 | 0.990 | 0.991 | 0.991 | 0.989 |
| multiBridge | 0m | 0.935 | 0.790 | 0.957 | 0.938 | 0.983 | 0.935 | 0.992 | 0.984 |
| | 5m | 0.958 | 0.883 | 0.977 | 0.958 | 0.992 | 0.968 | 0.996 | 0.992 |
| | 10m | 0.964 | 0.830 | 0.985 | 0.964 | 0.994 | 0.947 | 0.998 | 0.994 |
| rectCurve | 0m | 0.886 | 0.893 | 0.907 | 0.886 | 0.963 | 0.969 | 0.973 | 0.963 |
| | 5m | 0.909 | 0.910 | 0.908 | 0.915 | 0.974 | 0.977 | 0.974 | 0.974 |
| | 10m | 0.921 | 0.923 | 0.911 | 0.922 | 0.975 | 0.977 | 0.977 | 0.975 |
| spiral | 0m | 0.740 | 0.756 | 0.774 | 0.740 | 0.913 | 0.930 | 0.938 | 0.913 |
| | 5m | 0.776 | 0.812 | 0.809 | 0.776 | 0.927 | 0.946 | 0.948 | 0.927 |
| | 10m | 0.745 | 0.788 | 0.795 | 0.745 | 0.918 | 0.950 | 0.952 | 0.918 |
| square | 0m | 0.745 | 0.751 | 0.794 | 0.745 | 0.934 | 0.920 | 0.944 | 0.934 |
| | 5m | 0.751 | 0.778 | 0.830 | 0.752 | 0.932 | 0.928 | 0.959 | 0.932 |
| | 10m | 0.744 | 0.716 | 0.801 | 0.743 | 0.935 | 0.893 | 0.944 | 0.935 |
| star | 0m | 0.887 | 0.901 | 0.914 | 0.887 | 0.968 | 0.977 | 0.980 | 0.968 |
| | 5m | 0.903 | 0.899 | 0.916 | 0.900 | 0.974 | 0.977 | 0.982 | 0.974 |
| | 10m | 0.902 | 0.778 | 0.909 | 0.902 | 0.974 | 0.924 | 0.981 | 0.974 |
| Brooklyn Bridge | 0m | 0.378 | 0.542 | 0.490 | 0.378 | 0.888 | 0.930 | 0.925 | 0.888 |
| | 5m | 0.442 | 0.604 | 0.579 | 0.440 | 0.900 | 0.943 | 0.941 | 0.900 |
| | 10m | 0.504 | 0.639 | 0.581 | 0.507 | 0.915 | 0.950 | 0.944 | 0.915 |
| Brooktrail | 0m | 0.441 | 0.431 | 0.421 | 0.440 | 0.742 | 0.765 | 0.756 | 0.742 |
| | 5m | 0.476 | 0.512 | 0.489 | 0.475 | 0.750 | 0.825 | 0.800 | 0.750 |
| | 10m | 0.387 | 0.555 | 0.498 | 0.387 | 0.712 | 0.852 | 0.799 | 0.711 |
| Eiffel Tower | 0m | 0.397 | 0.481 | 0.492 | 0.397 | 0.851 | 0.882 | 0.898 | 0.851 |
| | 5m | 0.459 | 0.566 | 0.571 | 0.459 | 0.868 | 0.906 | 0.921 | 0.868 |
| | 10m | 0.411 | 0.553 | 0.553 | 0.411 | 0.861 | 0.907 | 0.923 | 0.861 |
| LAX | 0m | 0.557 | 0.607 | 0.593 | 0.557 | 0.867 | 0.898 | 0.905 | 0.867 |
| | 5m | 0.591 | 0.667 | 0.584 | 0.591 | 0.883 | 0.921 | 0.903 | 0.883 |
| | 10m | 0.485 | 0.590 | 0.637 | 0.479 | 0.857 | 0.903 | 0.925 | 0.857 |
| Laicheng | 0m | 0.768 | 0.807 | 0.804 | 0.768 | 0.857 | 0.874 | 0.874 | 0.857 |
| | 5m | 0.761 | 0.815 | 0.808 | 0.761 | 0.856 | 0.878 | 0.905 | 0.856 |
| | 10m | 0.773 | 0.823 | 0.809 | 0.773 | 0.861 | 0.880 | 0.911 | 0.861 |
| Skylawn | 0m | 0.618 | 0.822 | 0.733 | 0.618 | 0.871 | 0.956 | 0.927 | 0.871 |
| | 5m | 0.642 | 0.690 | 0.807 | 0.642 | 0.877 | 0.899 | 0.955 | 0.877 |
| | 10m | 0.729 | 0.703 | 0.822 | 0.729 | 0.927 | 0.905 | 0.957 | 0.927 |
| Stelvio Pass | 0m | 0.640 | 0.715 | 0.717 | 0.656 | 0.945 | 0.962 | 0.963 | 0.946 |
| | 5m | 0.739 | 0.791 | 0.768 | 0.739 | 0.962 | 0.974 | 0.975 | 0.962 |
| | 10m | 0.686 | 0.798 | 0.766 | 0.686 | 0.953 | 0.975 | 0.978 | 0.953 |
| Zhangjiajie | 0m | 0.760 | 0.832 | 0.799 | 0.760 | 0.964 | 0.978 | 0.976 | 0.964 |
| | 5m | 0.772 | 0.868 | 0.839 | 0.772 | 0.967 | 0.987 | 0.982 | 0.967 |
| | 10m | 0.835 | 0.911 | 0.873 | 0.835 | 0.978 | 0.991 | 0.990 | 0.978 |

Table 2: The number of cases with maximum NMI/Rand for each clustering algorithm

| # of cases | Max NMI | Max Rand |
|---|---|---|
| DBSCAN | 1 | 0 |
| ADCN-Eps | 25 | 19 |
| ADCN-KNN | 33 | 41 |
| OPTICS | 1 | 0 |

## List of Figures

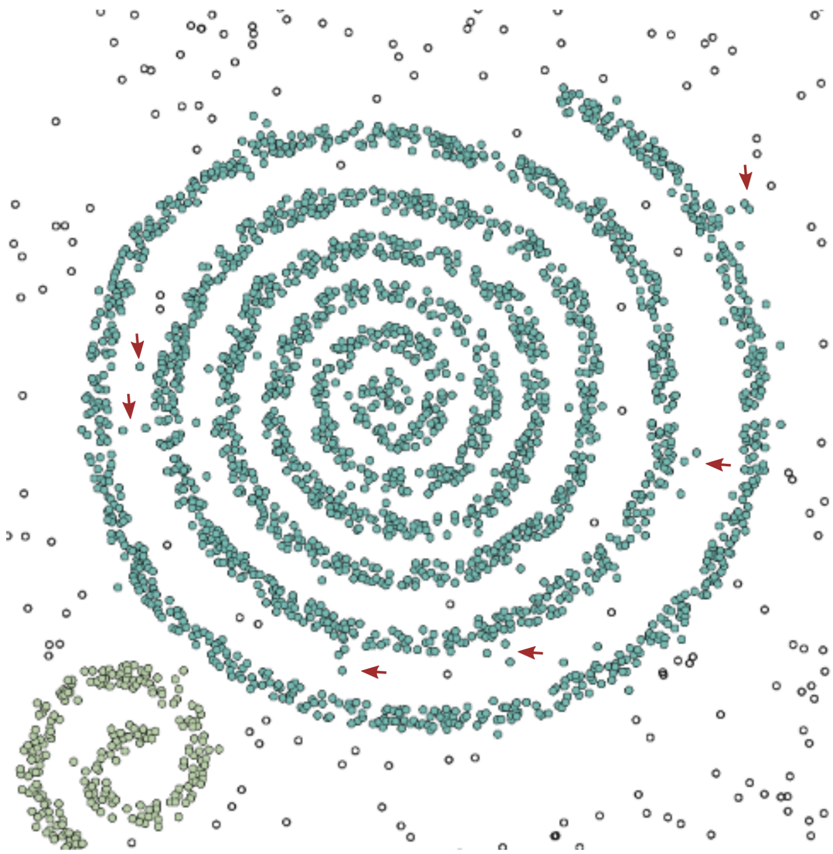

Figure 1: A spiral pattern clustered using DBSCAN. Some noise points are indicated by red arrows.

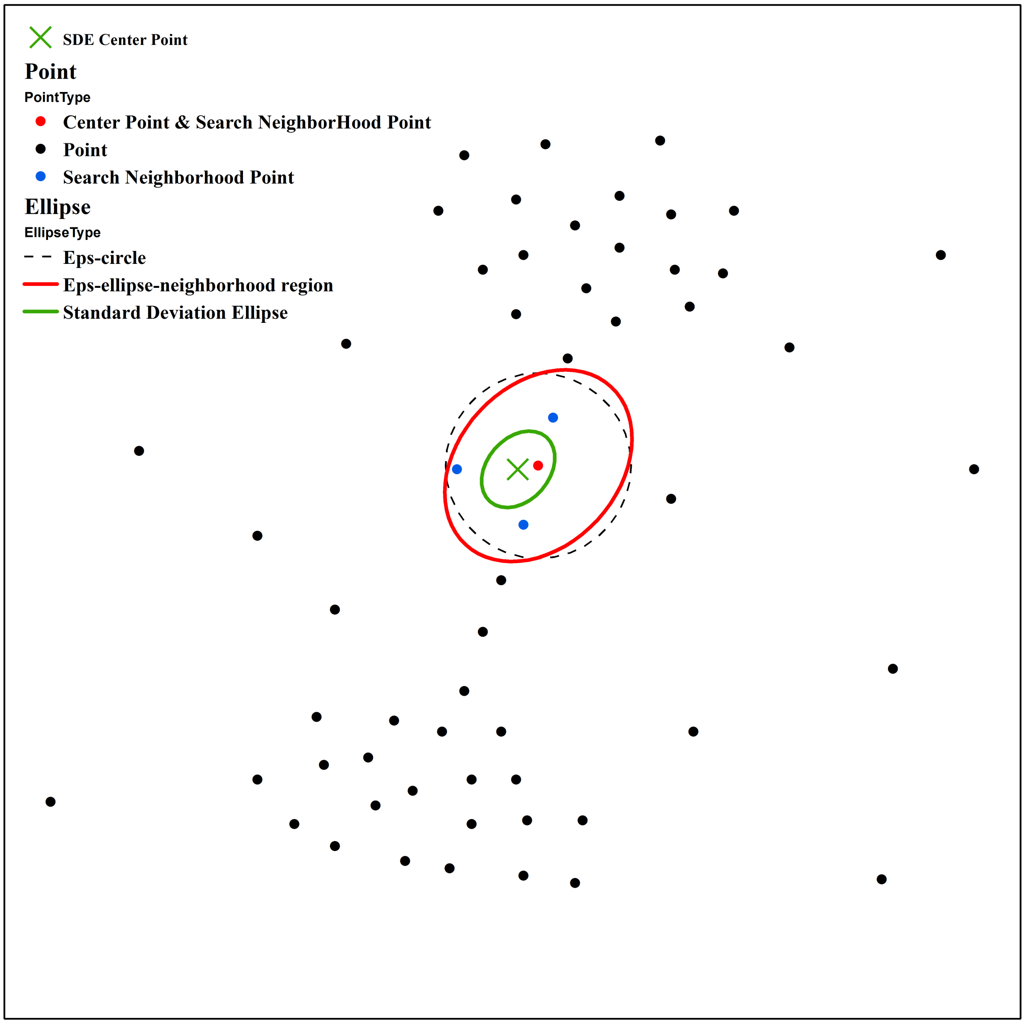


Figure 2: Illustration for ADCN-Eps

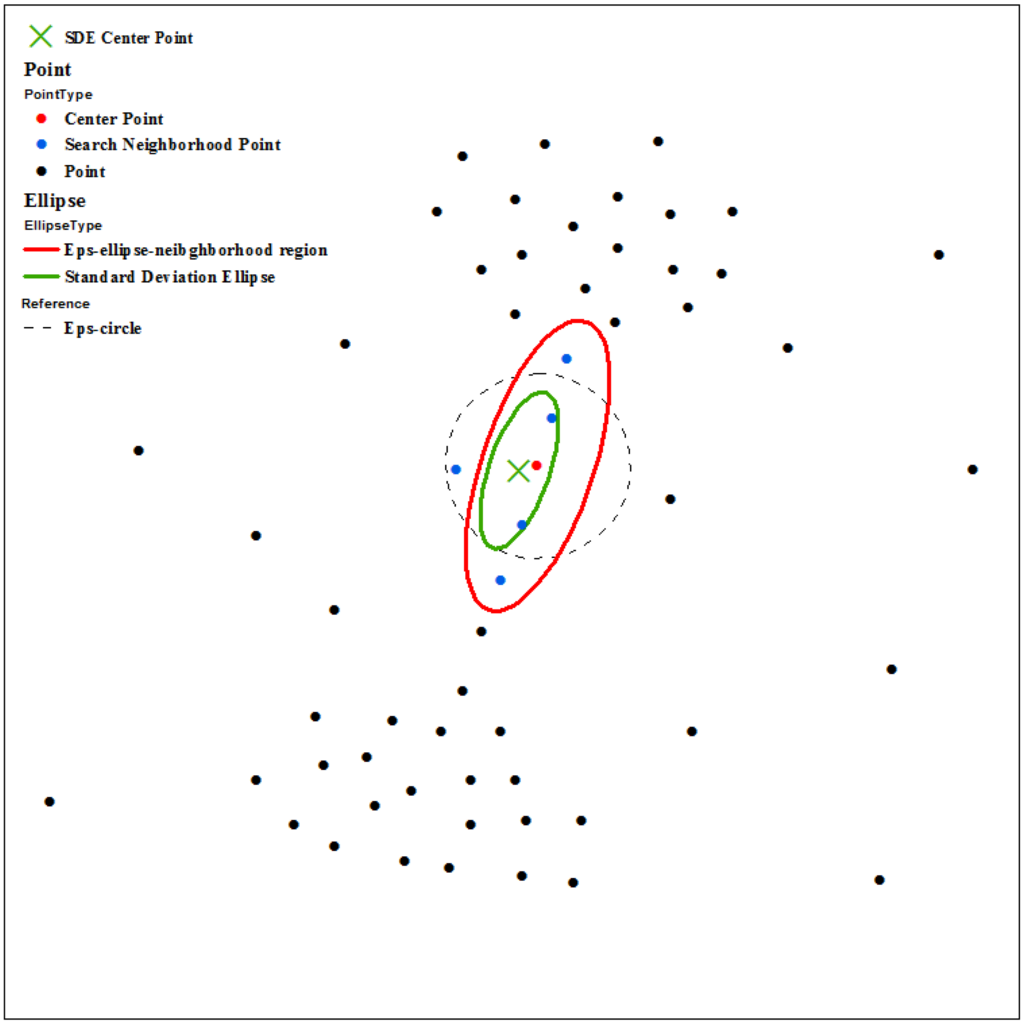


Figure 3: Illustration for ADCN-KNN

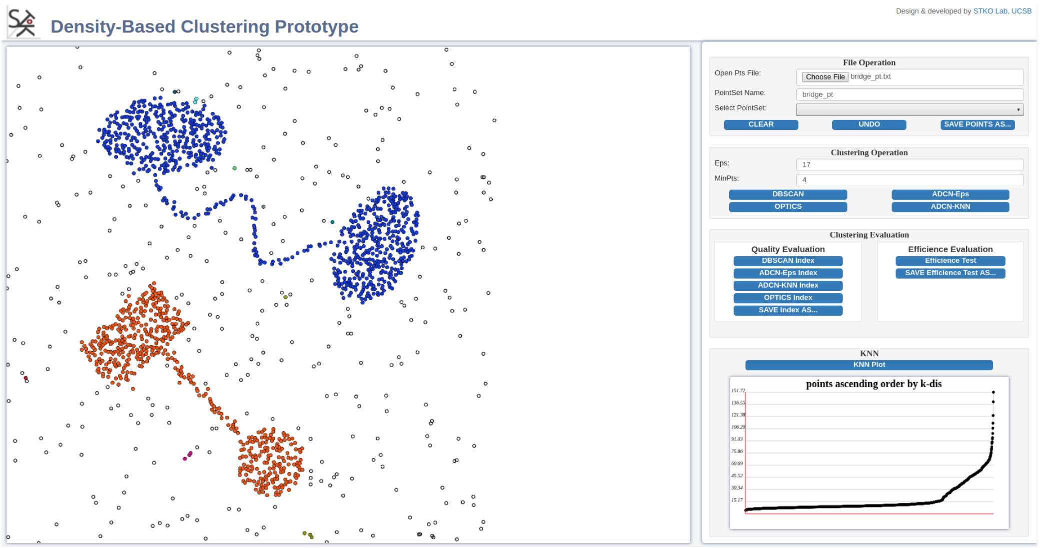


Figure 4: The Density-Based Clustering Test Environment

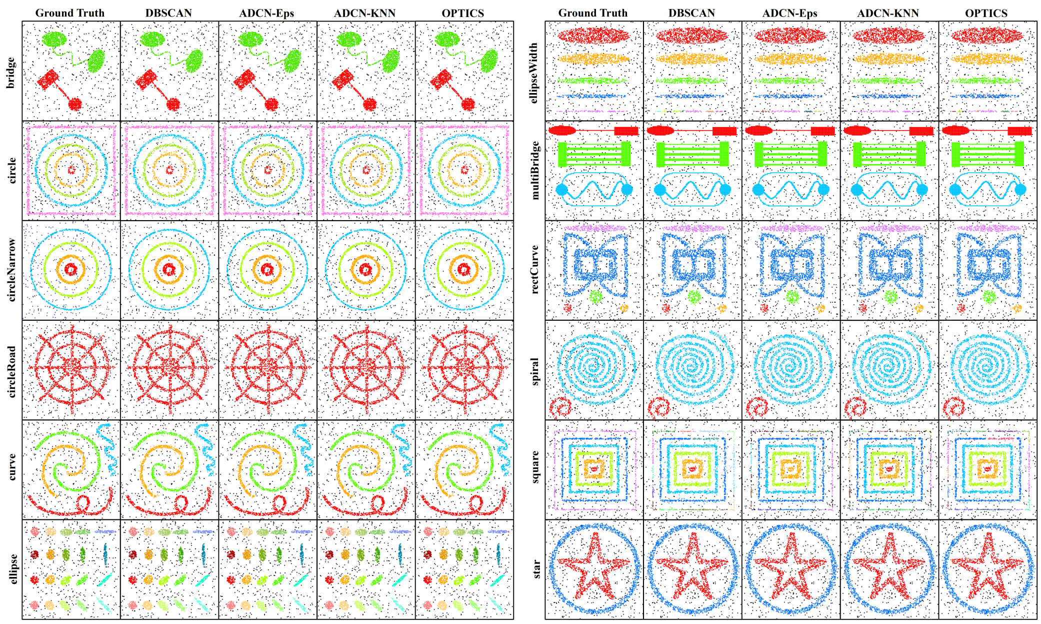


Figure 5: Ground truth and best clustering result comparison for 12 synthesis cases.

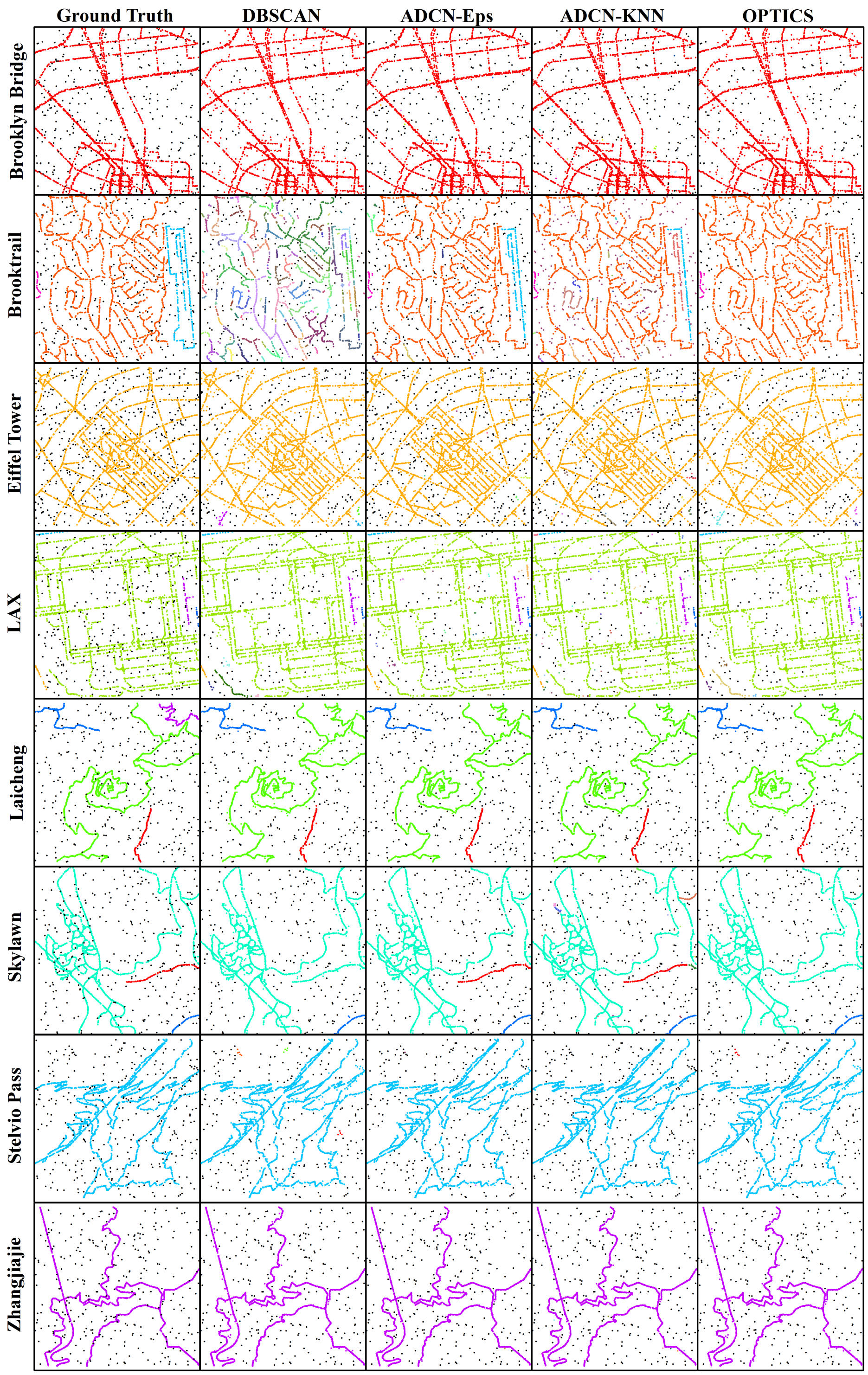




Figure 6: Ground truth and best clustering result comparison for eight real-world cases.

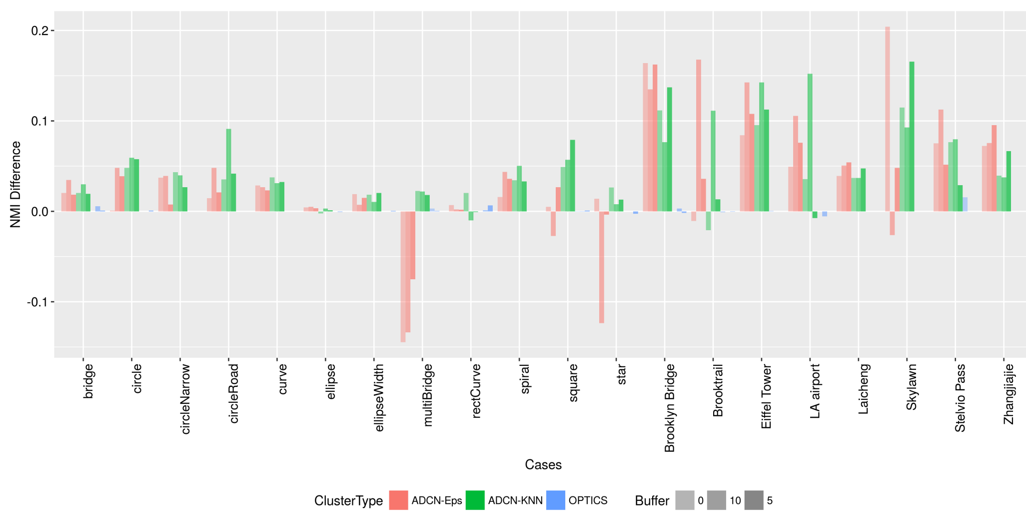


Figure 7: Clustering quality comparisons: NMI Difference between 3 clustering methods and DBSCAN for each case. Synthetic cases are on the left, real-world cases on the right.

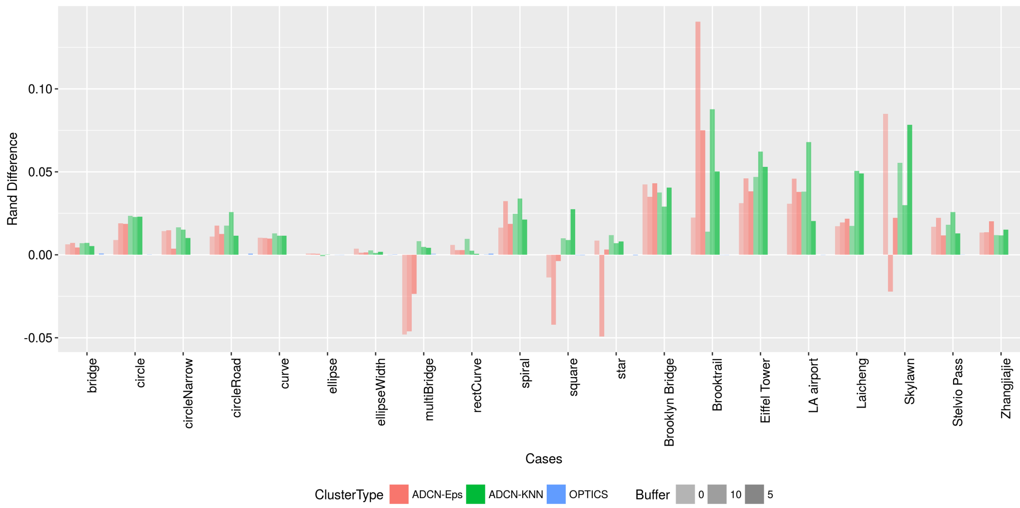


Figure 8: Clustering quality comparisons: Rand Difference between 3 clustering methods and DBSCAN for each case. Synthetic cases are on the left, real-world cases on the right.

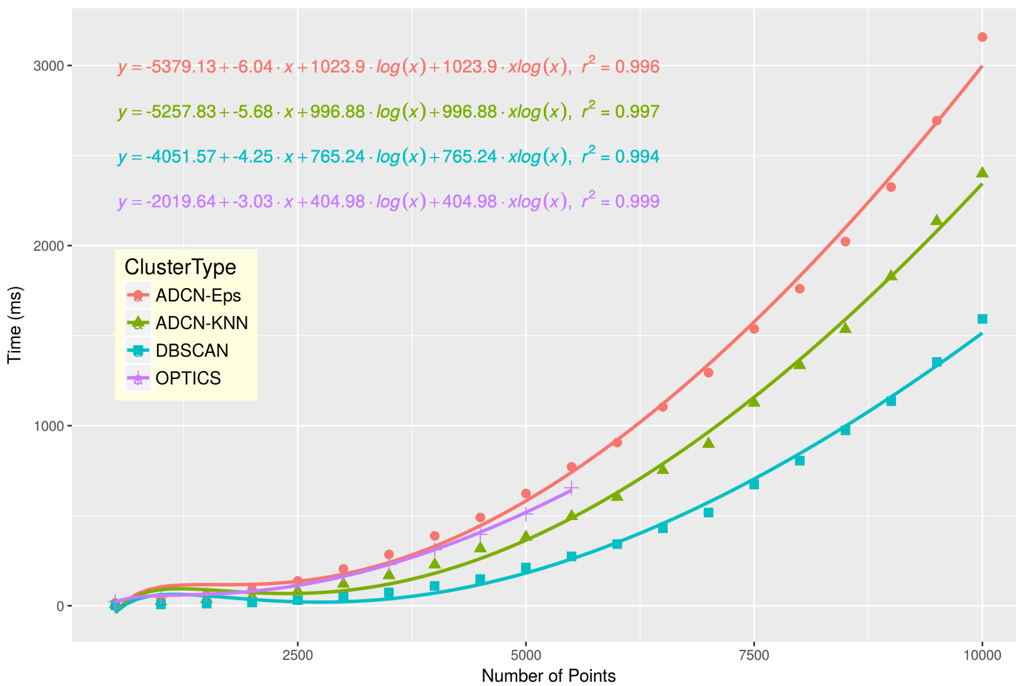


Figure 9: Comparison of clustering efficiency with different dataset sizes; runtimes are given in millisecond (The used OPTICS library failed on datasets exceeding 5500 points)